Title

Influence of sulphuric acid anodising on the fatigue strength of a 7075-T73 aluminium alloy

Authors

Savas, TP
Earthman, JC

Publication Date

2014

Peer reviewed

JMEPEG
DOI: 10.1007/s11665-014-1000-1

1059-9495/$19.00

Fatigue Crack Nucleation Studies on Sulfuric Acid Anodized 7075-T73 Aluminum

Terence P. Savas and James C. Earthman

(Submitted December 5, 2013; in revised form March 4, 2014)

The influence of a sulfuric acid anodic coating process on the fatigue crack nucleation behavior of 7075-T73 aluminum alloy was investigated. Silicone surface replication in combination with carbon sputter coating and scanning electron microscopy (SEM) allowed for in situ monitoring of the number of cycles for crack nucleation. A single edge circular notch (SECN) coupon was designed for the present study to localize fatigue damage thus enhancing fatigue crack detection and capture the effects of multiaxial stress conditions indicative of a majority engineering applications. Linear elastic finite element modeling of the SECN coupon was performed to quantify the von Mises equivalent stress distribution and the stress concentration factor of the notched region. The experimental results indicate that the presence of localized pitting corrosion initiated during the anodic coating pretreatment process had an adverse effect on fatigue performance. Specifically, multiple crack nucleation sites were evident as opposed to a single crack origin for the untreated specimens. Post-cycling SEM surface examinations displayed networks of micro-cracks in the anodic coating emanating from the pits although these were not found to be fatigue crack origin sites during post SEM fractographic exams. Thus, the stress concentration effect of the corrosion pits was found to be predominant. The total cycles to failure on average was reduced by approximately 60% for the anodic coated versus untreated specimens. A strategy is also discussed on how to mitigate accelerated crack nucleation by controlled surface pretreatment and use of a chromated chemical conversion coating in lieu of an anodic coating for selective applications.

Keywords 7075-t73, alodine, aluminum, anodic films, anodizing, chemical conversion coating, fatigue crack nucleation, pitting corrosion, pretreatment solutions, scanning electron microscopy

1. Introduction

The effects of preexisting corrosion pits, anodic coatings, and a combination of the two on the fatigue performance of high strength aluminum alloys have been studied extensively by previous investigators. Specifically with respect to the anodic coating it is well understood that since the anodic layer grows out of the substrate material and adheres extremely well to the base material that cracks in the anodic layer can accelerate fatigue crack nucleation (Ref 1-4). The thicker the coating the more pronounced this effect. Additionally while a sealed anodic coating improves the corrosion resistance it has been shown to fracture at lower strains compared to an unsealed coating and consequently further reduces fatigue strength. In either case, fatigue crack nucleation can be accelerated by cracks forming in the coating under applied strains and higher crack densities are known to occur with higher strain amplitudes (Ref 3).

The focus of the present work is on the surface topography produced on 70750-T73 aluminum alloy during a standard anodic coating process and how these features influence fatigue crack nucleation. A recent literature survey has yielded several related studies. For example, Pao et al. reported on the effect of preexisting corrosion pits on the crack nucleation kinetics of 7000-series high strength aluminum alloys of varying temper conditions. In this case, the specimens were exposed to a 336-h salt spray test to initiate the pits. It was reported that presence of the pits not only reduced the fatigue crack nucleation lives by a factor of two to three at the same stress level, but more importantly, lowered the fatigue crack nucleation stress thresholds by half (Ref 5). In a similar study Dolley et al. examined the effects of pitting corrosion on a 2024-T3 aluminum alloy. It was stated that corrosion pits acted as preexisting flaws in the material to nucleate fatigue cracks and the reduction in fatigue life was strongly correlated to the initial pit size. In this case, a fracture mechanics approach was used for probabilistic life determination with good correlation to the initial pit size. It was concluded that fatigue life was reduced significantly as compared to the untreated specimens and post scanning electron microscopy (SEM) examinations of the fracture surfaces revealed that all the cracks nucleated at the corrosion pits (Ref 6).

Genel studied environmental effects on the fatigue behavior of bare and anodic-coated 7075-T6 aluminum alloy (Ref 7). In this case smooth specimens were tested in both laboratory air and 3.5% NaCl solution. It was reported the presence of corrosive attack on the bare specimens drastically reduced fatigue performance primarily in the high cycle fatigue regime.

Terence P. Savas, Aerospace Group, Control Systems Division, Parker Hannifin Corporation, Irvine, CA 92618-1898 and Department of Chemical Engineering Materials Science, University of California Irvine, Irvine, CA 92697-2575: and **James C. Earthman**, Department of Chemical Engineering & Materials Science, University of California Irvine, Irvine, CA 92697-2575. Contact e-mails: tsavas@parker.com and earthman@uci.edu.

Published online: 18 April 2014

For example, the fatigue strength of the bare specimens was a factor of 2.9 lower than the coated specimens with a film thickness of 23 μm that showed only a modest reduction in fatigue strength.

Specific to the effects of anodic coating processes that create corrosion pits in the pretreatment steps and during the anodic coating process itself, Shazad et al. examined the influence of pickling and chromic acid anodizing processes on 7050-7451 aluminum alloy. It was reported that in the high cycle fatigue regime the fatigue strength of the (1) pickled specimens and (2) pickled and anodized specimens was reduced by 32 and 43%, respectively. Post-fracture SEM analyses showed that a large majority of cracks initiated at preexisting corrosion pits and very few from strain cracks in the coating for the anodized specimens. Based on the fractographic exams it was also noted that the decrease in fatigue life was due to a combination of the effects of pitting and multi-site nucleation (Ref 8). Additional studies by the same researchers on pickled and anodized 7010-T451 further confirmed the deleterious effects of pitting defects on fatigue performance (Ref 9). Specifically it was found that the pickling solution predominantly attacked grain boundaries and intermetallic inclusions resulting in surface artifacts that acted as crack initiation sites as revealed during post-fracture SEM examinations.

More recently Baohua et al. (Ref 10) reported on the very high cycle fatigue life degradation due to chromic and sulfuric acid treatments on 2A12-T4 aluminum alloy. Interestingly for the chromic acid process, it was discovered that the fatigue cracks imitated at the interface between the film and substrate due to tensile stresses created by the elastic mismatch as opposed to the sulfuric acid process where segmentation cracks in the film and overgrowth of the film into the surface was the primary crack nucleation mechanism.

The present authors reported on the influence of the following categories of solutions on the localized corrosion behavior of 7075-T73 aluminum including: liquid degreasing, non-etching alkaline cleaners, high pH caustic cleaners, low pH acid-based deoxidizers, and a low pH sulfuric acid solution (as part of the electrochemical anodizing process itself). Specimens were exposed to various solutions and combinations of solutions to better understand their corrosive affects with one specimen going through a complete anodize process. It was concluded that the designated category-1 and -2 solutions did not cause any corrosion damage while the category-3 and -4 solutions did. Specifically, the category-3 high pH caustic etch solution was the most aggressive resulting in severe general and localized attack after short exposure times in the 60-120 s range. The low pH deoxidizer solution also caused general attack and localized pitting corrosion was present after 600 s exposure; however, this solution was much less aggressive than the caustic etch. The larger pits (on the order of 10-20 μm) that were initiated during the pretreatment processes did grow in size during the subsequent electrochemical anodic coating process. For the smaller pits (on the order of 1-5 μm) the anodic process had a smoothing effect where the film growth tended to passivate the pits (Ref 11, 12).

An important consideration regarding engineering design and application is that most published fatigue data is generated using coupons with a polished and uncoated surface finish. Although this appears to be good practice for generating design data with minimized scatter, it is not indicative of typical manufactured industrial components (in service) or those going through qualification testing that requires some form of corrosion protection. In addition, the surfaces are generally not polished as this would become cost prohibitive. The available data in the open literature are also limited with respect to the material product form and temper. For example, the Metallic Materials Properties Development and Standardization (MMPDS) Handbook (Ref 13) contains the engineering properties and related characteristics of wrought and cast aluminum alloys used in aircraft and missile structural applications. This specification is typically flowed down as a contractual requirement for fatigue design of airborne equipment. Although this source data is widely accepted among prime aircraft manufacturers for use in mechanical design it does not include fatigue data for type 7075 alloy in the hand-forged product form in the overaged (T73) temper condition. Additionally, the surface finishes of the fatigue coupons in MMPDS are either polished or unspecified. Another commonly used alloy in airborne applications is Type 2219 aluminum alloy. Here the MMPDS only provides fatigue data for 5.08-cm (2.0 in.)-thick plate stock; however, Type 2219 material is commonly used for applications requiring thick hand forgings up to 43 cm (17 in.).

There is a significant amount of fatigue data for type 7075 forgings in the T73 temper condition reported in the literature (Ref 14). However, the forgings are not specified to be open die (hand) or closed die, and information regarding surface finishes and the location in the forging from where the coupons are extracted is not provided. Other disadvantages of published smooth specimen SN data include the inability to clearly distinguish between crack nucleation and crack propagation stages of fatigue failure (Ref 13, 14). Quantifying the cycles to crack nucleation is of particular importance in parts with thick wall sections since the crack propagation cycles may contribute significantly to the overall fatigue life. Because of these limitations in the referenced handbook data accurate fatigue life analyses continue to pose a significant challenge to design and structural engineers.

The specific objectives of the present study were as follows: (1) develop a test coupon that localizes fatigue damage to one location to assist with crack nucleation detection and captures the effect of multiaxial stress conditions indicative of a majority engineering applications, (2) fabricate and process the fatigue coupons (both untreated and anodized) with the processing steps clearly defined herein, (3) perform three dimensional linear elastic finite element modeling to quantify the von Mises equivalent stress and the stress concentration factor at notched region of the coupon, (4) perform uniaxial fatigue tests along with SEM surface replication for crack detection on bare (untreated) coupons and anodic-coated coupons to gain a comprehensive understanding on the effects of preexisting corrosion pits and the anodic layer on fatigue crack nucleation kinetics and (5) perform post-cycling SEM examinations to identify the fracture initiation sites.

It should be noted that a relatively small quantity of coupons were used for the present experiments. As such, the intent was not to generate fatigue life (SN) data that could be used for design purposes but rather help define future research efforts and help articulate to the scientific community and industry the need for a standardized fatigue data base generated more closely under simulated service conditions. For example, anodic-coated fatigue coupons with surface finishes indicative of standard manufacturing processes. Preferably these results would be widely accepted as source data for the design of critical (airborne) components by prime, subprime, and lower level original equipment manufacturers (OEM) with the ultimate goal of better correlating handbook data to application.

2. Experimental Procedures

2.1 Material

The as-received material consisted of a 7075-T73 aluminum alloy hand-forged billet (Ref 15) with a 0.152 m (6 in.) square cross section and a length of 0.381 m (15 in.). To obtain the 7075 in a stabilized (overaged) T73 temper condition, the billet was solution heat treated at 471 °C (880 °F) for 7 h, water quenched at room temperature, artificially aged for 6 h a 107 °C (225 °F), and stabilized for 8 h at 177 °C (350 °F). The chemical compositions and mechanical properties of the alloy are provided in Tables 1 and 2, respectively, for the specific heat lot used in this study. In addition, for this specific heat lot, a comprehensive microstructural analysis using SEM and energy dispersive spectroscopy (EDS) was used for second phase (constituent) particle identification. Second phase particles were shown to induce pitting corrosion during solution exposure (Ref 11).

2.2 Fatigue Coupon Design

To localize fatigue damage and thus facilitate crack nucleation detection a single edge circular notch (SECN) geometry was developed for the present study. The notch and associated stress concentration factor (Kt) was indicative of those commonly found in engineering applications. A schematic of the SECN specimen is illustrated in Fig. 1.

An important consideration taken into account in this study was the raw material thickness and the area from the hand forging from which the coupons are extracted. This consideration is needed for thick sections since the thermomechanical working history of the raw material directly influences the size and distribution of microporosity, quench efficiency, effectiveness of the subsequent precipitation hardening response, and grain size. All these microstructural attributes directly impact fatigue behavior. For example, it was shown that uniaxial fatigue testing of smooth coupons machined from a thin plate stock compared to those machined from a thick hand forging could provide an increase in fatigue life of up to two orders of magnitude for the same high strength aluminum alloy (Ref 16-19). To account for this variation the coupons for the present study were extracted from the center ($T/2$) section of the hand-forged billet as illustrated in Fig. 2 thus representing a worst-case microstructure and hence a conservative approach for interpreting the data.

Another important consideration for the present specimen geometry was that elevated shear stresses produced by the lack of constraint at sharp corners generally lead to crack initiation at these corners. To avoid initiation at the corner of the notch the corners were rounded to a radius of 0.76 mm (0.030 in.). A finite element model was to assure that the shear stresses, represented by the von Mises equivalent stress were reduced at the notch corners as described in the following section.

2.3 Finite Element Modeling

Finite element modeling (FEM) was conducted on the SECN coupon geometry to accurately determine the stress distributions at the notched region. The finite element code COSMOS© Design Star Version 4.0, developed by Structural Research and Analysis Corporation, was used in the present analysis. Three-dimensional linear elastic FEM was performed on the coupon geometry using nominal dimensions as specified on the engineering drawing. The stresses in the model were evaluated using an applied load of 2224 N (500 lbs). The model consisted of ten-noded tetrahedral solid elements with a with a element size of 0.076 mm (0.003 in.) in the local stress critical (notch) region and 1.09 mm (0.043 in.) for the global elements. This element size was verified to be accurate as finer mesh density models converged to predict same level of stress. The model predicted a maximum von Mises equivalent stress across the face of the notch of 196.5 MPa (28.5 ksi) with the 2224 N (500 lbs) applied axial load at the pin joints. The net section (P/A) stress was calculated as 73.8 MPa (10.7 ksi). A ratio of the maximum local stress and the net section (P/A stress) resulted in a stress concentration factor (Kt) of 2.65 for this configuration. Figure 3 illustrates a close-up mesh density view of the coupon FEM.

2.4 Surface Processing

The following sulfuric acid anodic coating process was implemented for the SECN coupons. This is a typical process in accordance with Ref 20. Note that Ref 20 is a general guideline used in the industry and is therefore flexible in requirements to account for various materials, part geometry, and as-received part conditions. For example, a part with severe heat treat scale or oxide can require much more aggressive pretreatments prior to anodizing. However, the process defined below is indicative of machined aluminum components with generally a clean (as-received) surface.

2.5 Fatigue Testing

The fatigue testing was conducted on the SECN coupons in a Mechanical Testing Systems (MTS) servohydraulic fatigue testing machine in accordance with the methods defined in ASTM E467—Conducting Constant Amplitude Axial Fatigue Tests of Metallic Materials. All tests were conducted in laboratory air using a sinusoidal waveform at a frequency of 3 Hz and a load ratio of $R = 0.1$. A total of 15 SECN coupons were tested at various stress levels of which six were sulfuric acid anodized in accordance with Table 3. Also note the runout stress level was only established for the untreated coupons. These coupons did not fail as the testing was stopped for logistical purposes.

3. Results

Surface replication was conducted at various intervals of the fatigue testing. The data presented herein are limited to crack nucleation observations for two samples (i.e., untreated and anodic coated). In this study, crack nucleation was defined as a

Table 1 Chemical composition (wt.%) for 7073-T73 alloy evaluated in the present study

Alloy Type	Cu	Fe	Si	Mn	Mg	Zn	Cr	Ti	Zr	V	Al
7075	1.5	0.26	0.07	0.020	2.4	5.6	0.19	0.02	…	…	Bal

Table 2 Mechanical properties for 7075-T73 alloy evaluated in the present study

Alloy type	Grain direction	Yield strength MPa (ksi)	Tensile strength MPa (ksi)	% Elongation
7075-T73	Longitudinal	381.3 (55.3)	460.5 (66.8)	15
	Long-transverse	368.9 (53.5)	449.5 (65.2)	12.5
	Short transverse	402.7 (58.4)	477.2 (69.2)	7

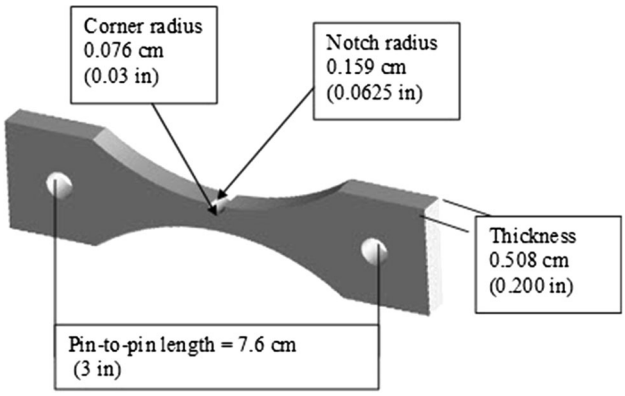

Fig. 1 Schematic of SECN fatigue coupon used for the present study

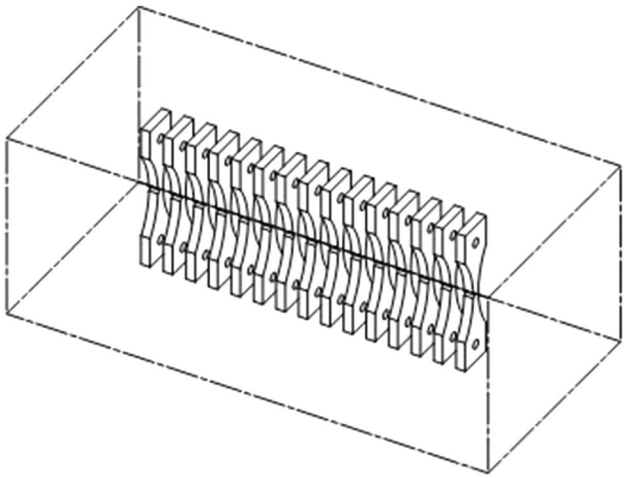

Fig. 2 Schematic of hand-forged billet with *T*/2 location of extraction of coupon gage section

size that could be detected using standard NDT techniques (e.g., dye penetrant) on the order of 0.127 to 0.254 mm (0.005 to 0.010 in.). As expected from the finite element results shown in Fig. 3, crack initiation was not observed at the corners of the notch in each specimen. Rather, cracks nucleated on the interior face of the notch confirming the validity of the finite element predictions. SEM surface replication is shown in Fig. 4 for the untreated (as-machined) condition with zero fatigue cycles. Figure 5 illustrates a surface replica taken at 44,000 cycles with evidence of a single primary crack origin. This sample ultimately failed at 68,880 cycles with load amplitude of 3080 N (692 lbs). This loading condition produced a maximum cyclic stress level of 273 MPa (40 ksi) at the notch root. The primary fatigue crack shown measured to be approximately 150 μm (0.006 in.) at the time of recording.

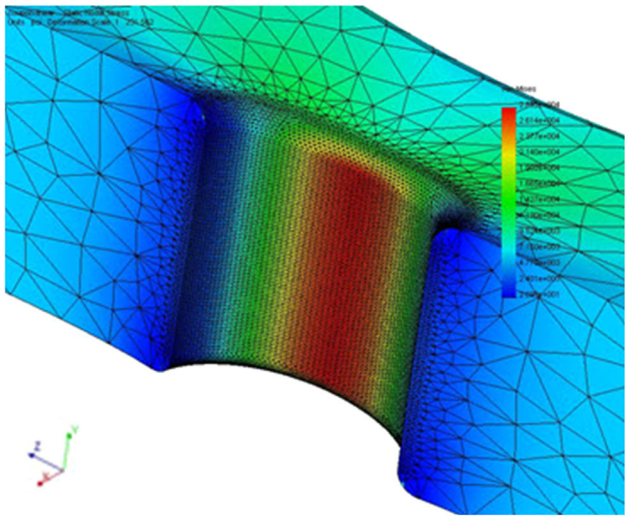

Fig. 3 Close-up view of SECN fatigue coupon FEM. Maximum von Mises equivalent stress at notch section calculated to be 19.7 MPa (28.5 ksi) with a 2224 N (500 lbs) load applied

Figure 6 shows a surface replica taken from the anodized coupon gage section at zero cycles. Note a significant population of preexisting corrosion pits initiated during the anodic coating pretreatment process is evident. As hypothesized in Ref 11 if the pits initiating during the pretreatment exposures were beyond a threshold size (on the order of 10-20 μm) a higher current density existed at these locations during subsequent electrochemical processes, thus resulting in larger and deeper pit structures. For smaller pits (on the order of 1-5 μm) the anodic process had a smoothing affect where the film growth tended to passivate the pits.

Figure 7 illustrates the same surface taken after 21,623 fatigue cycles. This anodized coupon failed at 38,985 cycles with load amplitude of 2800 N (630 lbs). This loading condition produced a maximum cyclic stress level of 266 MPa (39 ksi) at the notch root. Note that multiple origin fatigue cracks nucleating at the corrosion pits are clearly evident. Figure 8 shows a large primary fatigue crack (annotated with arrow in Fig. 7). Figure 8 also shows networks of strain cracks in the anodic coating emanating from the pit origins.

Figure 9 shows an SEM photomicrograph of a failed coupon. It can be seen (as with other coupons examined) the fatigue crack nucleation site is a preexisting corrosion pit. Crack arrest lines can also been seen that are an artifact of stopping the fatigue cycling for intermittent surface replication. The nucleation site is centered about the radial arrest lines further substantiating this defect as the origin. Adjacent pitting defects can also be observed in the upper left side of the photo.

Although the results presented herein present two specimens, replica data at lower and higher stress levels proved similar trends with respect to accelerated and multiple fatigue crack nucleation. Figure 10 shows the cumulative results for

Table 3 Sulfuric acid anodic coating process implemented for the present study

Solution type/temperature	Category	Exposure time
Water rinse/22 °C (72 °F)	…	120 s
Liquid degreaser/71 °C (160 °F)	1 (a)	600 s
Water rinse/22 °C (72 °F)	…	120 s
Alkaline cleaner 71 °C (160 °F)	2 (a)	600 s
Water rinse/22 °C (72 °F)	…	120 s
Caustic etch 71 °C (160 °F)	3 (b)	120 s
Water rinse/22 °C (72 °F)	…	120 s
Deoxidizer/22 °C (72 °F)	4 (c)	120 s
Water rinse/22 °C (72 °F)	…	120 s
Type-II anodize 22 °C (72 °F)	5 (d)	1800 s
Water rinse/22 °C (72 °F)	…	120 s
Seal/DI water 93 °C (200 °F)	6	900 s

(a) Solutions prepared as a 10% aqueous solution of liquid concentrate (Brulin Corp). (b) Solution prepared by mixing 30 g/L NaOH, solid granulated form (Diversey Corp). (c) Solution prepared as a 10% aqueous solution of $HNO_3 + Fe_2(SO_4)_3$ liquid concentrate (Chemetall Oakite Corp). (d) Solution prepared as 15% aqueous solution of sulfuric acid (H_2SO_4) and processed in accordance with (Chemtall Oakite Corp)

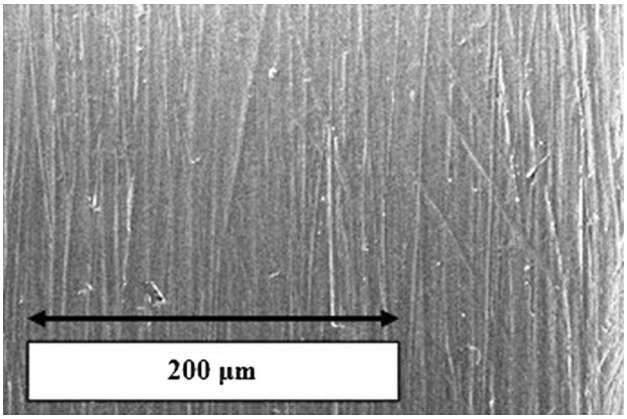

Fig. 4 SEM replication at notch root of untreated sample at zero cycles (×300)

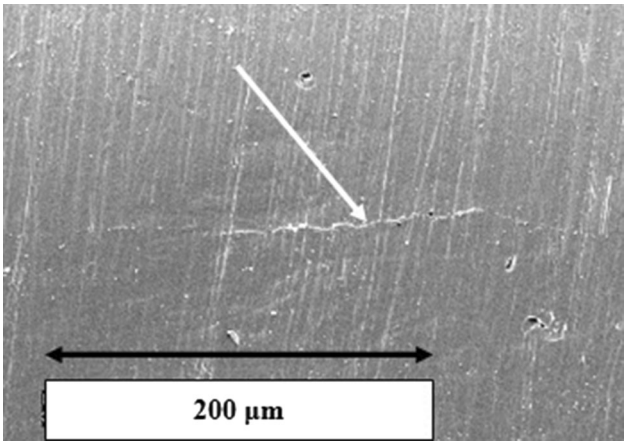

Fig. 5 SEM replica taken at notch root of untreated sample at 44,000 cycles (×300). Note single origin fatigue crack (approximate length of 150 µm) annotated by white arrow

the present study in terms of stress reversals versus cycles to failure. Results indicate a notable reduction in fatigue life up to 60% for the anodic coated versus untreated coupons. Generally

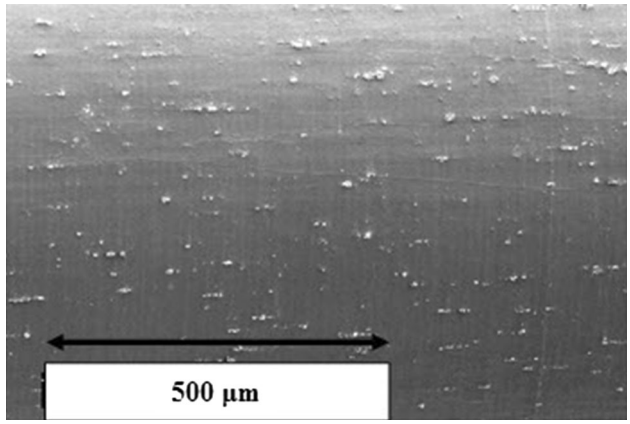

Fig. 6 SEM replica taken at notch root of anodized sample at zero cycles. Note high density of pits initiated during the anodic pretreatment process (×100)

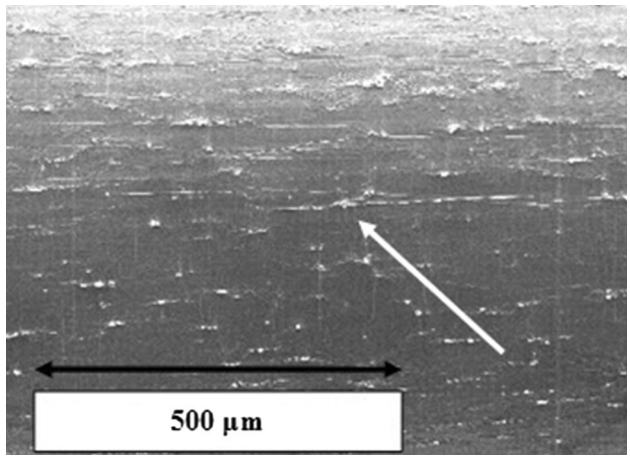

Fig. 7 SEM replica taken at notch root of anodized coupon at 21,000 cycles (×100). Note high density (multiple origin) fatigue cracking nucleating at preexisting pits (largest crack annotated by white arrow)

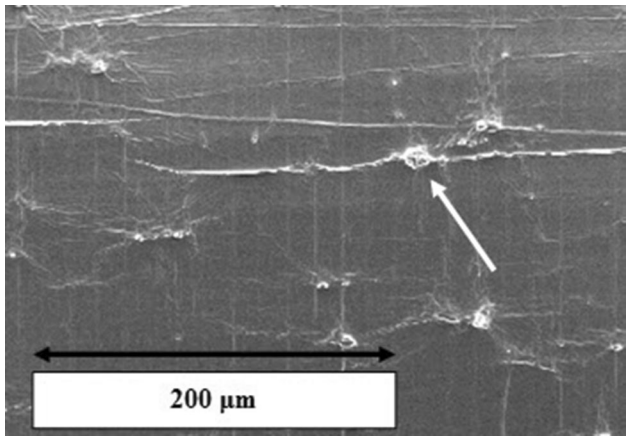

Fig. 8 Close up view of large crack identified by white arrow in Fig. 9 (×300). Also note high density of strain cracks in the coating emanating from the pit origins

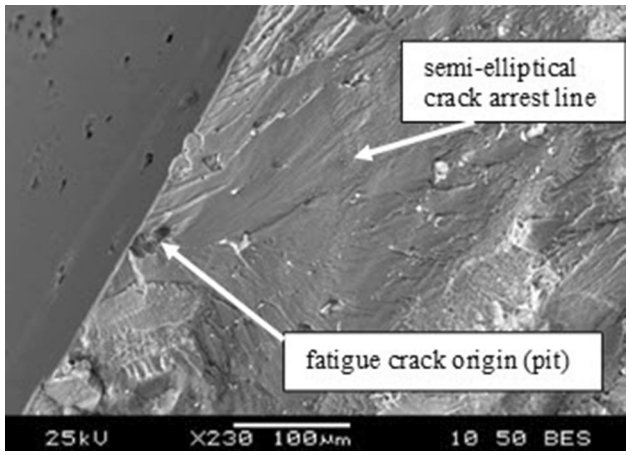

Fig. 9 Fracture surface morphology of failed coupon. Note typical pit structure acting as crack nucleation site and semi-elliptical crack arrest line (×230)

at all stress levels crack nucleation occurred at approximately 50% of the overall fatigue life. This substantiates the importance of distinguishing between cycles to crack initiation (Ni) and cycles of crack propagation (Np) and reiterating that most published SN data does not distinguish between the two.

4. Discussion

The present results indicate that corrosion pits resulting from an anodizing treatment reduced the fatigue life of 7075-T73 aluminum specimens by 60%. This finding is in good agreement with previous researchers utilizing similar materials and processes (Ref 5-9). In addition, the findings for the present study are consistent with those using analytical methods to model and predict crack nucleation and crack growth. For example, Rokhlin et al. (Ref 21) developed a three-dimensional fracture mechanics model to study fatigue crack initiation and growth from artificial pits. The model showed very good agreement with experiments in predicting the dependence of reduction of fatigue life as a function of pit size.

To potentially minimize the adverse effects on fatigue performance associated with pretreatments and anodizing—a chemical conversion coating approach, i.e., alodine (Ref 22) can be implemented. This strategy would be applicable (although not limited to) to parts or assemblies that are (a) subsequently painted for corrosion protection and/or (b) are a pressure vessel or similar device that may for example contain a corrosion inhibiting liquid such as a petroleum-based hydraulic fluid.

The experience of the present authors indicates that chemical conversion coatings can be successfully applied to various 2000- and 7000-series wrought aluminum alloys with minimum surface pretreatments. The surface pretreatments can be limited to a liquid-based (detergent) degreasing solution followed by a mild non-etching alkaline soak cleaner and a final water rinse. However, it should be verified that the mild cleaning process is able to produce a chemically clean (water break free) surface which is an absolute prerequisite for a successful chromated chemical conversion process. This approach can potentially reduce the risks of localized corrosion and excessive surface roughening found with more aggressive pretreatments. It should be noted that the mild (non-etching) cleaning method may not be effective for as-heat treated, scaled surfaces, or highly contaminated surfaces, for example, those with embedded contaminants such as dirt and oxides. Each part, fabrication history and service conditions require an individual assessment.

After a chromated chemical conversion treatment followed by a chromate-primer (Ref 23) and a polyurethane paint (Ref 24) application samples were exposed to a 336 h SO_2 salt-fog environment tested in accordance with the ASTM G 85, Standard Practice for Modified Salt Spray (Fog) Testing, Annex A4. After exposure and paint removal the surface was confirmed to have no evidence of corrosive attack. Results for these experiments indicated the corrosion resistance of painted aluminum alloys is not strongly dependent on the underlying surface treatment, for example, chemical conversion or various types of anodic coatings. It was reported that the chromate-based primer provides a primary means of corrosion protection and the base metal pretreatments are of secondary importance in aggressive high humidity sulfuric and hydrochloric acid (salt-fog) environments. Similar results were published by the Naval Air Warfare Center for painted Type-I chromic acid and Type-IIB thin-film sulfuric acid anodized 7075 and 2024 alloys. It was reported that the painted corrosion resistance in neutral salt-fog and SO_2/salt-fog environments was largely dependent on the paint scheme and less on the underlying pretreatment or alloy (Ref 25).

A specific example to consider is hydraulic flight control manifold assemblies for naval aircraft applications. These are routinely externally coated with primer and paint. In this case the internal passages and most internal aluminum components are continuously wetted by hydraulic fluid that is consistently shown to inhibit various types of corrosion including galvanic and localized forms. A chemical conversion coating in lieu of an anodic coating where appropriate can provide several advantages. Specifically for fatigue critical hydraulic manifolds machined from wrought aluminum, surface pretreatments can be limited to the non-etching type thus reducing the risk of localized corrosion damage than can accelerate fatigue crack nucleation. Secondly, exclusion of anodic films will eliminate the risks of strain cracks forming in the film, for example, under proof pressure applications that have also been shown to accelerate fatigue crack nucleation. An alodine-only approach can potentially reduce the degree of surface roughening

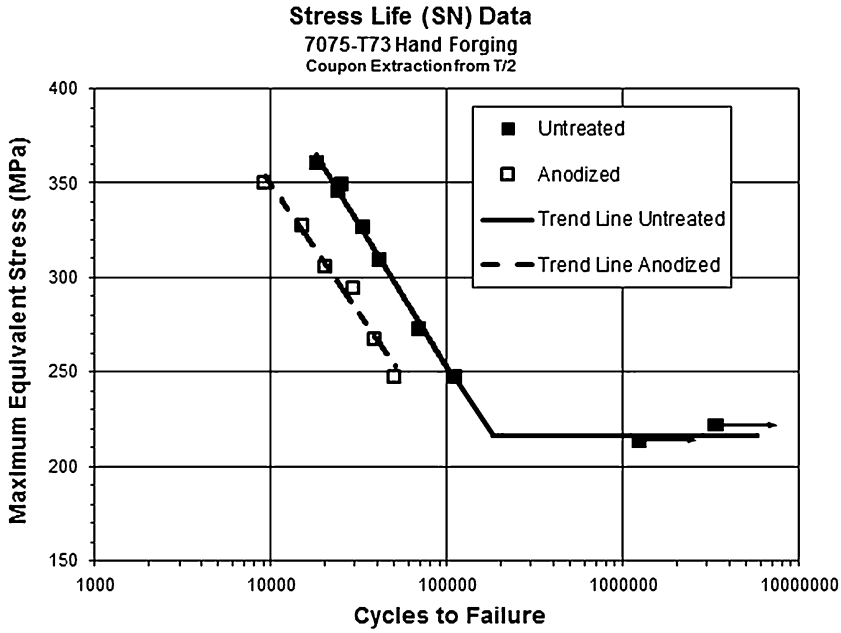

Fig. 10 Stress life (SN) data for the present study. Note an approximate 60% reduction in life is observed for the anodic coated vs. untreated coupons

associated with anodic coatings attributed to etching type pretreatments, corrosion defects, and cracked films. This is particularly important for leakage critical applications since experience has shown that hydraulic fluid can leak past elastomeric sealed surfaces where excessive roughness or localized pitting and intergranular corrosion can exist.

A final consideration with respect to coating processes is cost. Most hydraulic applications require that many areas of a manifold housing (or similar components) be alodined for electrical bonding purposes. Therefore, significant labor goes into masking complex shapes that require alodine in some areas and anodize on the remainder. It was recently reported for a fairly complex manifold housing that there is a tenfold increase in processing costs to go from 100% alodine to external anodize with internal passages and cavities alodined. One disadvantage of an alodine-only approach is the surface will have less abrasion resistance and may be more susceptible to handling or mating part galling damage. In the latter case, proper uses of dry film lubricants, anti-seize compounds, or wet lubricants such as hydraulic fluid can be used to mitigate these risks.

5. Conclusions

The influence of a sulfuric acid anodic coating process on the fatigue crack nucleation behavior of 7075-T73 aluminum alloy was examined in the present study. To facilitate the experiments a novel SECN coupon was designed to localize fatigue damage thus enhancing fatigue crack detection and capturing the effects of multiaxial stress conditions indicative of a majority engineering applications. FEM was also performed on the coupon geometry for accurate determination of the stresses and stress concentration factor at the notched gage section. The purpose of the fatigue testing was not to create SN data that could be used for design purposes but rather understand the adverse effects of the preexisting corrosion defects on crack nucleation mechanisms and to compare these results to the behavior of untreated specimens. SEM surface replication at predetermined intervals of loading cycles was implemented for this purpose.

These results emphasized the fact that the corrosion defects significantly accelerated fatigue crack nucleation. The fatigue cracks were indeed found to nucleate at the pit locations that were in high concentration on the treated surfaces (refer Fig. 7 and 8). It is evident by fractographic examinations that the presence of these defects circumvents classical Stage-1 fatigue nucleation by alternating slip band growth. Based on the samples tested, fatigue life was decreased by up to 60% for the anodic-coated coupons as compared to the untreated coupons (Fig. 10). The results of the present investigation clearly indicate the adverse effects of pretreatment and anodic coating processes on fatigue crack nucleation behavior. Additionally, the results are in close agreement with previous investigators on the crack nucleation mechanisms and the overall reduction in fatigue life.

Acknowledgment

The financial support of Parker Aerospace, Irvine, California, is gratefully acknowledged.

References

1. G.W. Stickley, Additional Studies of Effects of Anodic Coatings on the Fatigue Strength of Aluminum Alloys, *ASTM Proc.*, 1960, **60**, p 577–588
2. G.W. Stickley and J.O. Lyst, Effects of Several Coatings on Fatigue Strengths of Some Wrought Aluminum Alloys, *J. Mater.*, 1966, **1**(1), p 19–33
3. W.G.J. Hart and A. Nederveen, The Influence of Different Types of Anodic Layers on the Fatigue Properties of 2024-T3 and 7075-T6, National Aerospace Laboratory (NLR), Amsterdam, Netherlands, Report # NLR TR 80077 U, July 1980

4. L.S. Sharp, G.E. Nordmark, and C.C. Menzemer, *Fatigue Design of Aluminum Components & Structures*, McGraw Hill, New York, 1996
5. P.S. Pao, S.J. Gill, and C.R. Feng, On Fatigue Crack Initiation from Corrosion Pits in 7075-T7351 aluminum alloy, *Scr. Mater.*, 1998, **43**(5), p 391–396
6. E.J. Dolley, B. Lee, and R.P. Wei, The Effect of Pitting Corrosion on Fatigue Life, *Fatigue Fract. Eng. Mater. Struct.*, 2000, **23**, p 555–560
7. K. Genel, Environmental Effect on the Fatigue Performance of Bare and Oxide Coated 7075-T6 Alloy, *Eng. Fail. Anal.*, 2013, **32**, p 248–260
8. M. Shahzad, M. Chaussumier, R. Chieragatti, C. Mabru, and F. Rezai-Aria, Surface Characterization and Influence of Anodizing Process on Fatigue Life of Al 7050 Alloy, *Mater. Des.*, 2011, **32**(6), p 3328–3335
9. M. Shahzad, M. Chaussumier, R. Chieragatti, C. Mabru, and F. Rezai-Aria, Influence of Anodizing Process on Fatigue Life of Machined Aluminum Alloy, *Proc. Eng.*, 2010, **2**, p 1015–1024
10. N. Baohua, Z. Zheng, Z. Zihuai, and Z. Qunpeng, Effect of Anodising Treatment on the Very High Cycle Fatigue Behavior of 2A12-T4 Aluminum Alloy, *Mater. Des.*, 2013, **50**, p 1005–1010
11. T.P. Savas and J.C. Earthman, Surface Characterization of 7075-T73 Aluminum Exposed to Anodizing Pretreatment Solutions, *J. Mater. Eng. Perform.*, 2008, **17**(5), p 674–681
12. T.P. Savas and J.C. Earthman, Corrosion of Type 7075-T73 Aluminum in a 10% HNO3 + $Fe_2(SO_4)_3$ Solution, *J. Mater. Eng. Perform.*, 2009, **18**(2), p 196–204
13. *Metallic Materials Properties Development and Standardization (MMPDS)*, Chapter 3, Re-issue 7, December 2012
14. ASM International, *Fatigue Data Book: Light Structural Alloys*, ASM International, Materials Park, 1995
15. AMS-A-22771, Aluminum Alloy Forgings, Heat Treated, *SAE International*, June 1999
16. R.J. Bucci, R.W. Bush, A.J. Hinkle, H.J. Konish, M. Kulak, R.H. Wygonik, G.W. Kuhlman, and E.D. Seaton, Property/Performance Attributes of Forgings, *AeroMat'95, ASM International's 6th Advanced Aerospace Materials & Processes Conference*, Anaheim, CA, May 8–11, 1995
17. P.E. Magnusen, R.J. Bucci, A.J. Hinkle, and R.L. Rolf, Durability Assessment Based on Initial Material Quality, *J. Test. Eval.*, 1990, **18**, p 439–445
18. P.E.Magnusen, R.J. Bucci, A.J. Hinkle, J.L. Rudd, Fatigue Durability Improvement in Thick Section Metallic Airframe Parts, White Paper, ALCOA Technical Center, August 1992
19. P.E. Magnusen, R.J. Bucci, A.J. Hinkle, and R.L. Rolf, The Influence of Material Quality on Airframe Structural Durability, *7th International Conference on Fracture*, Houston, TX, March 20–24, 1995
20. Military Specification—Mil-A-8625, Anodic Coatings for Aluminum and Aluminum Alloys, Department of Defense, April 25, 1988
21. S.I. Rokhlin, J.Y. Kim, H. Nagy, and B. Zoofan, Effect of Pitting Corrosion on Fatigue Crack Initiation and Fatigue Life, *Eng. Fract. Mech.*, 1998, **62**, p 424–444
22. Military Specification—Mil-C-5541, Chemical Conversion Coatings on Aluminum and Aluminum Alloys, Department of Defense, November 30, 1990
23. Military Specification—Mil-PRF-23377H, Primer Coatings: Epoxy, High Solids, Type-I, Class-C, Department of Defense, April 30, 2002
24. Military Specification—Mil-PRF-85285D, Coating: Polyurethane, Aircraft and Support Equipment, Type-I, Class-H, Department of Defense, June 28, 2002
25. S.M. Cohen and S.J. Spadafora, A Comparison of Thin Film Sulfuric Acid Anodizing and Chromic Acid Anodizing Processes, Naval Air Warfare Center Aircraft Division, Report No. NAWCADWAR-95023-43, April 25, 1995